



The Consequence of the Involvement of Flexural, Compression, and Punching Reinforcement Upon Punching Strength

Ahmed Abdallah Elgoahry ^{1*} , Mohammed Rabiee ¹

¹ Department of Structural Engineering, Cairo University, Cairo, Egypt.

Received 07 May 2024; Revised 18 August 2024; Accepted 24 August 2024; Published 01 September 2024

Abstract

Flat slabs have an important role in concrete buildings due to their architectural flexibility and speed of construction. Punching shear is one of the most important phenomena to be considered during the design of reinforced concrete flat slabs, as this type of failure is brittle and does not predict previously raised alarms before failure. The main factors that affect punching strength in concrete are compressive strength, flexural reinforcement, and punching reinforcement in the form of stirrups, shear studs, or other shapes. This paper is part of a research program operated at the reinforced concrete laboratory of the Faculty of Engineering, Cairo University, to evaluate the contribution of horizontal flexural reinforcement, horizontal compression reinforcement, and vertical punching reinforcement on the punching strength of reinforced concrete flat slabs. In this research, fifteen half-scale specimens are cast and tested. The specimens had dimensions of 1100×1100 mm and a total thickness of 120 mm. All specimens were connected to a square column of dimensions 150×150 mm and loaded at the four corners with a supported span of 1000 mm. The main parameters considered in this research included spacing between stirrups, width of the stirrups, number of stirrup branches, ratio of the compression reinforcement, and ratio of the tension reinforcement. During testing, ultimate capacity, steel strain, cracking pattern, and deformation were recorded. The experimental results were analyzed and compared against values estimated from different international design codes.

Keywords: Punching; Flat Concrete Slabs; Longitudinal Steel; Punching Vertical Reinforcement; Crack Pattern; Load at Ultimate Stage.

1. Introduction

Punching shear failure in concrete slabs is a brittle failure and not ductile. This failure results from shear diagonal cracks formed by the overall slab thickness, which form a frustum pyramid in concrete rectangular columns and a trenched cone in concrete circular ones. Design standard codes deal with the punching failure problem in different ways. For example, the Egyptian Code of Practice E.C.P. 203–2020 [1] and the American Code ACI318-19 [2] highly underestimate the punching capacity due to neglecting the horizontal reinforcement in equations. While the European Code Euro-Code 2 [3] takes flexural reinforcement into consideration, in addition, the location of the critical section of punching varies among the design standard codes from half to double the effective slab depth measured from the concrete column face. The first analytical model presented to predict the punching behavior was the Kinnunen and Nylander model [4], which neglected the effect of longitudinal reinforcement on the punching capacity of concrete slabs.

The punching capacity can be increased by adding drop panels, concrete compressive strength, punching shear reinforcement, and bent-up bars. Strengthening existing slabs by using composite materials such as carbon fiber reinforced polymers (CFRP) and glass fiber reinforced polymers (GFRP) [5] enhances the punching strength. Ebead [6] tested existing slabs after strengthening with CFRP strips and GFRP laminates. The strips showed an average gain in

* Corresponding author: ahmed.202010021@eng-st.cu.edu.eg

 <http://dx.doi.org/10.28991/CEJ-2024-010-09-014>



© 2024 by the authors. Licensee C.E.J, Tehran, Iran. This article is an open access article distributed under the terms and conditions of the Creative Commons Attribution (CC-BY) license (<http://creativecommons.org/licenses/by/4.0/>).

punching capacity of 40% compared to the specimen without any strengthening. Moreover, flexural strengthening specimens using GFRP laminates showed an average increase in punching load capacity of 31% compared to that of unstrengthened slabs. Megally [7] performed tests on slab column connections subjected to concentric and seismic loads. He concluded that providing a slab with a drop panel increased the capacity without considerable improvement in ductility or energy absorption strength. Broms [8] proposed a combined system of stirrups and bent bars in order to discard the brittle punching failure of specimens. The author tested slabs and provided with bent bars as hangers into the concrete column, in addition to stirrup cages welded around the column. This concept was very effective for a ductile structural system. Out of the above-mentioned improvement systems, using flexural reinforcement in addition to stirrups proves to be the most practical method to be applied to enhance punching behavior.

Mabrouk et al. [9] studied the punching strength of seven half-scale column-slab specimens with the dimensions: 1050×1050 mm with a total thickness of 100 mm. The parameters consist of flexural reinforcement ratio, spacing between vertical stirrups, stirrup width, and the number of branches on the punching conduct of flat slabs. Adding vertical shear reinforcement in the form of stirrups improved the punching capacity of the slabs by 23% in the case of spacing 100 mm and by 36% in the case of spacing 50 mm. The flexural tensile reinforcement in a flat slab contributes to the punching strength of the slab. As the flexural reinforcement ratio increased by 45%, the punching capacity increased by 16% compared to the control specimen. More variables are investigated in the current research to evaluate the contribution of vertical stirrups, flexural reinforcement, and compression reinforcement in enhancing the punching behavior of flat slabs. Raafat et al. [10] proposed eight inner slab-column connections with varying slab depth, closed-shaped stirrups, several leg stirrups, yielding stress, and extended length. Punching capacity increased by 8.2% when the stirrups extended from the column's edge by more than twice the effective depth of the slab, and punching capacity was improved by increasing the thickness of the slabs.

The mix of concrete has an important role in punching strength. Abdel-Rahman et al. [11] tested fourteen slab-column connections in order to study the punching shear behavior of reinforced concrete slabs using steel fibers in the concrete mix. They concluded that the mode of failure of the tested specimens was brittle and sudden; increasing the steel fiber ratio increased punching shear capacity and improved both the initial and tangent slopes of the load-deformation curve.

Pre-stressed concrete has a positive improvement in punching strength at flat slabs. Afifi et al. [12] conducted a series of specimens with variable dimensions of concrete column and punching vertical reinforcement ratio on a concrete pre-stressed flat slab. The author predicted that both stiffness and ductility would improve due to the pre-stressed concrete slab. Ramadan et al. [13] conducted an experimental program to explore the effect of concrete compressive strength and the pre-stressing force on the punching strength of the ultra-high-performance concrete slabs. They observed that the increase in concrete compressive strength led to a delay in cracking before the brittle punching shear failure and significantly increased the punching shear strength with more ductile mode. Punching failure occurs in a way that makes the slab crack along critical areas that pass through the slab from its compression to tension zones in an inclined direction [14]. This failure is sudden; no apparent signs were observed before the failure. Hence, the dependable prediction of the punching shear capacity of slab-column connections is important in the design. It is important to note that the data used to develop any formula is limited to a portion of the studies carried out before the date of development. To obtain a reliable prediction for the punching shear capacity of RC slab-column connections, it is essential to have a comprehensive and updated dataset wherever accurate or modern prediction techniques are applicable.

Traditional experimental procedures are the established technique for evaluating the various characteristics of concrete elements [15]. Habibi et al. [16] conducted Models of Ensemble Learning for Prediction of Punching Shear Strength in RC Slab-Column Connections. The authors observed that the models are proposed for predicting punching shear strength.

2. Experimental Program

2.1. Experimental Specimens

Figure 1, shows the flowchart of the research methodology through which the objectives of this study were achieved. The testing program was conducted at the Cairo Engineering Laboratory, Egypt, for fifteen flat concrete slab specimens. The main aim of this research was to estimate the results of some parameters on punching behavior. The main parameters are longitudinal steel ratio at the tension side, compression reinforcement ratio, and vertical reinforcement with variable stirrup widths and a variable number of branches on the punching conduct of the tested slabs. The tested slab models had a size of 1100 mm length, 1100 mm width, and 120 mm in thickness, with a column dimension of 150×150×250 mm in the middle of the tested slabs. High-tensile-grade (500/650) steel deformed bars are used as a longitudinal reinforcement with a 12 mm diameter. In order to avoid flexural failure, additional reinforcement with a diameter 12 mm was added to all tested specimens at the tension zone. Mild reinforcement (240/350) with an 8-mm stirrup diameter was applied. Table 1 displays all of the specimen's details.

Group one is composed of five reinforced concrete specimens without vertical stirrups and without compression longitudinal reinforcement. The main parameter among this group was the longitudinal steel ratio at the tension side, as shown in Figure 2. The longitudinal steel proportion varied from 1.03% to 2.05%.

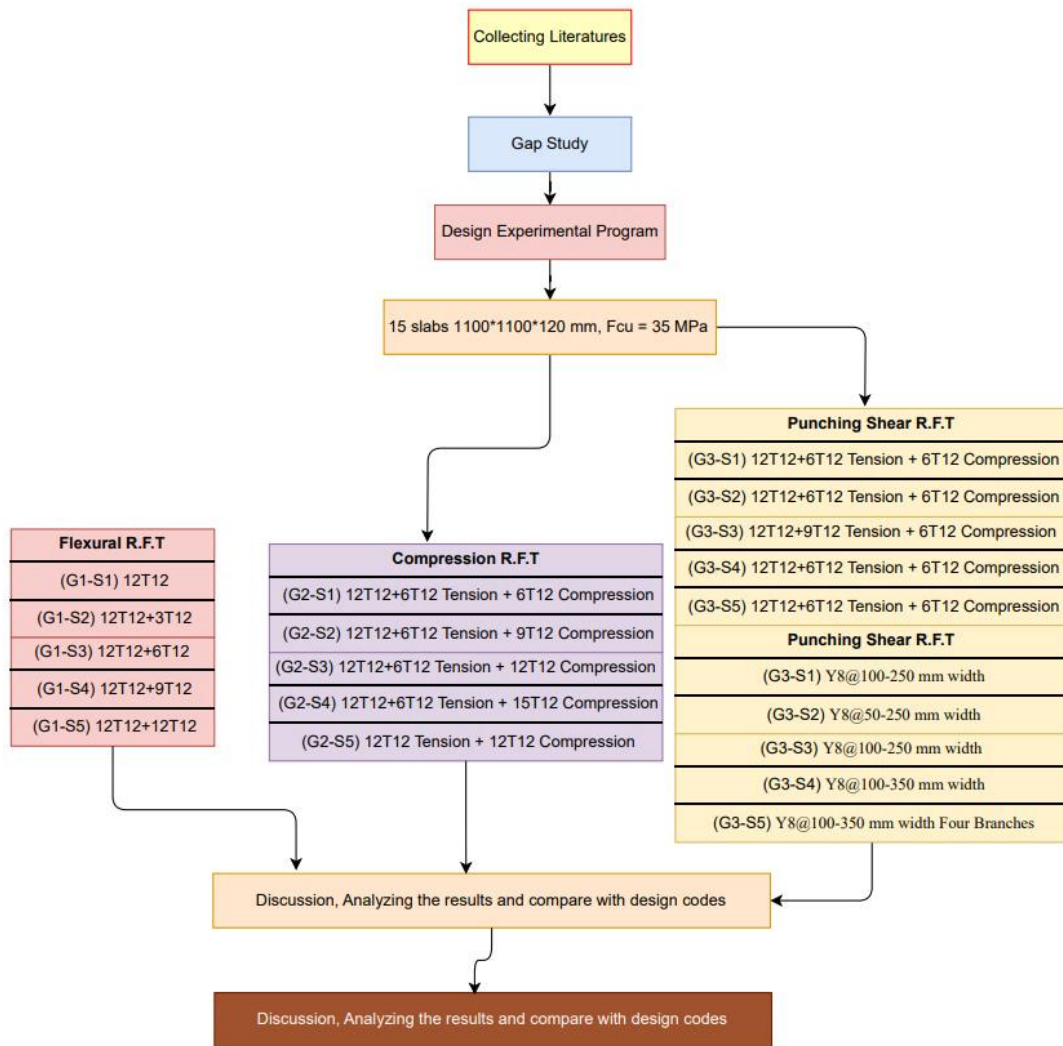


Figure 1. The considered methodology

Table 1. Properties of the tested specimens

Specimen	Tension reinforcement	Compression reinforcement	Punching shear reinforcement
G1-S1	12T12		
G1-S2	12T12+3T12		
G1-S3	12T12+6T12		
G1-S4	12T12+9T12		
G1-S5	12T12+12T12		
G2-S1	12T12+6T12	6T12	
G2-S2	12T12+6T12	9T12	
G2-S3	12T12+6T12	12T12	
G2-S4	12T12+6T12	12T12+3T12	
G2-S5	12T12	12T12	
G3-S1	12T12+6T12	6T12	Y8@100-250 mm width
G3-S2	12T12+6T12	6T12	Y8@50-250 mm width
G3-S3	12T12+9T12	6T12	Y8@100-250 mm width
G3-S4	12T12+6T12	6T12	Y8@100-350 mm width
G3-S5	12T12+6T12	6T12	Y8@100-350 mm four branches

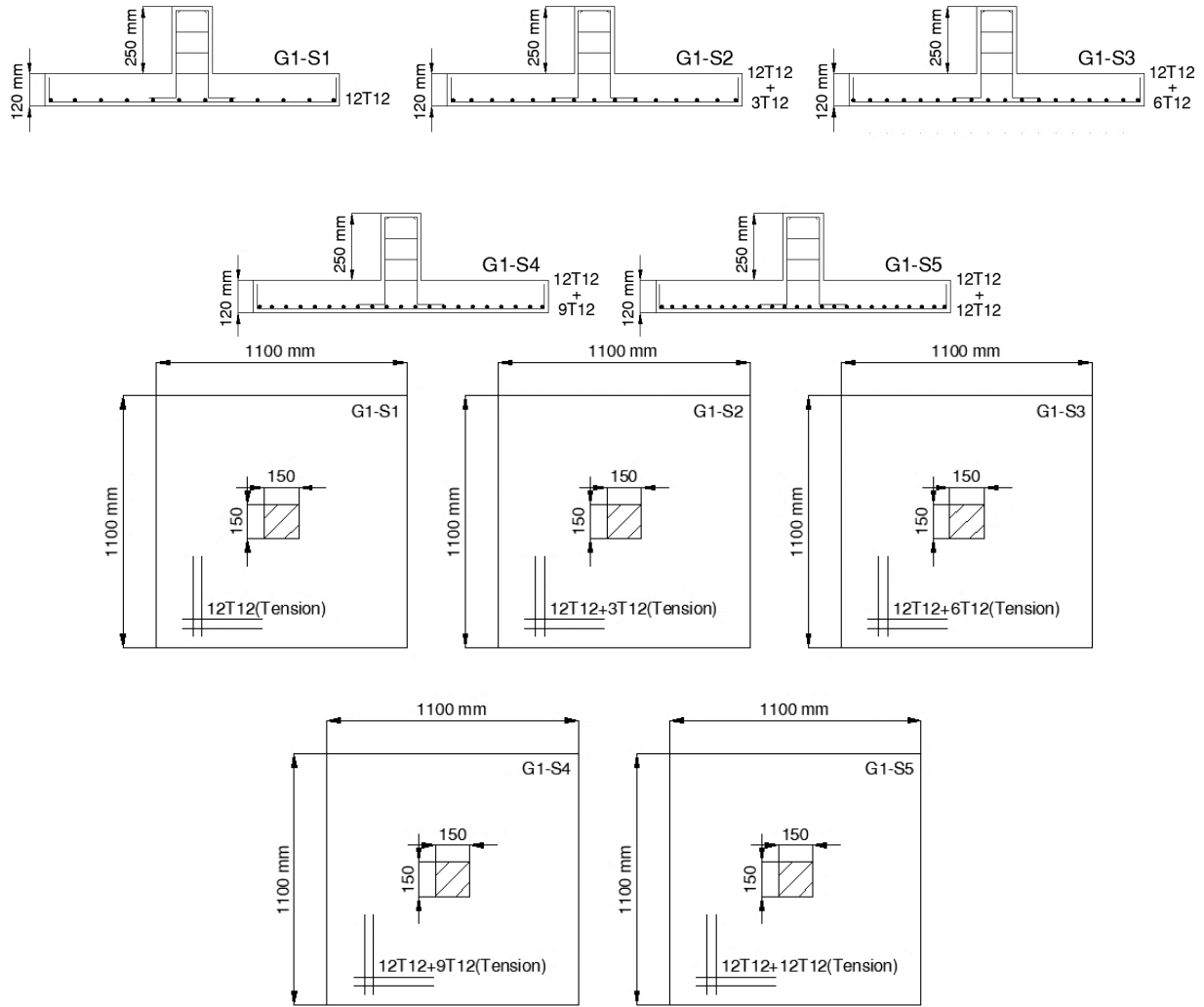
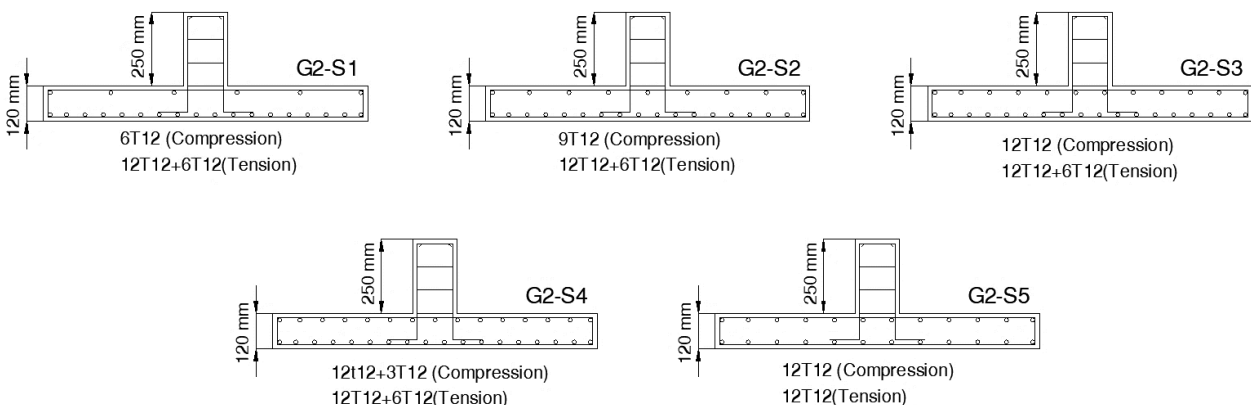


Figure 2. Specimens plan and sections details of group-1 (flexural reinforcement ratio)

The specific proportions of flexural reinforcement for the samples tested in this study were determined, and these proportions were based on common practices in the field of construction, such as the additional top reinforcement, which is in different proportions to resist moments at the columns, which is added to the concrete columns in flat slabs. Higher proportions of additional flexural reinforcement were also added to obtain more accurate results from the effect of flexural reinforcement on the punching shear strength.

Group two, this group is composed of five slabs without providing punching reinforcement. The main parameter in this group was compression reinforcement ratio as a percentage of flexural reinforcement, as shown in Figure 3, where compression reinforcement ratio was varied from 33 to 100% as a percentage of flexural reinforcement.



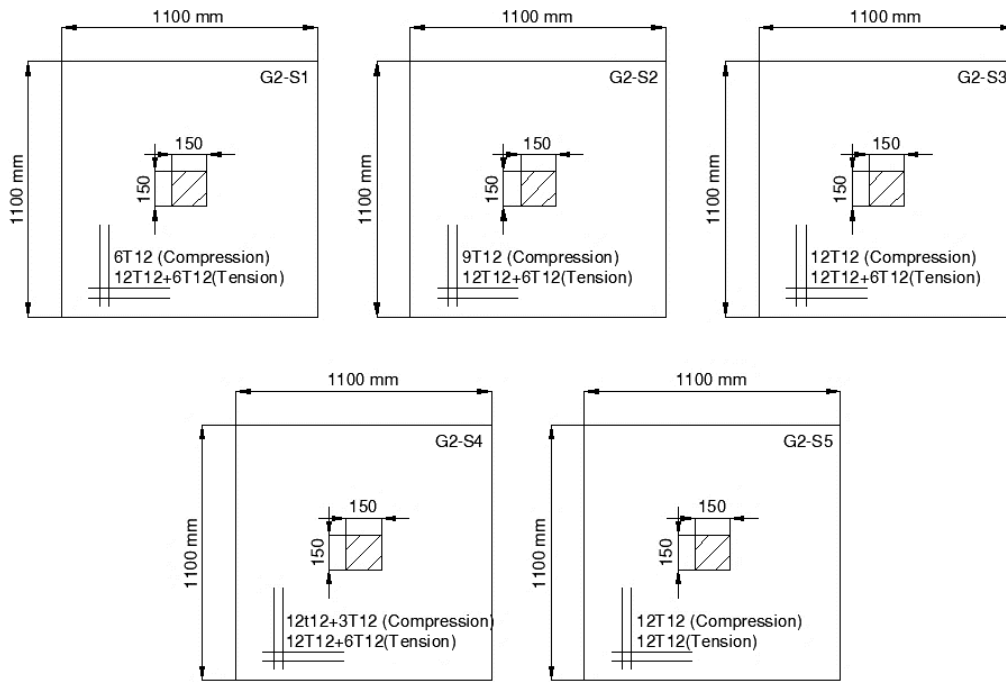


Figure 3. Specimens plan and sections details of group-2 (compression reinforcement ratio)

Group three, composed of five slabs, provides punching reinforcement with variable ratios, as shown in Figure 4, where the distance between stirrups and the number of branches are variable. The stirrups of specimens (G3-S1) and (G3-S3) were 8 mm in diameter, two branches with a width of 250 mm, and repeated at a distance of 100 mm. The stirrups of specimen (G3-S2) were 8 mm in diameter, two branches with a width of 250 mm, and repeated at a distance of 50 mm. The stirrups of specimen (G3-S4) were similar to specimen (G3-S1), but the stirrup width was 350 mm instead of 250 mm. The stirrups of specimen (G3-S5) were similar to specimen (G3-S4), but the stirrups were four branches instead of two branches.

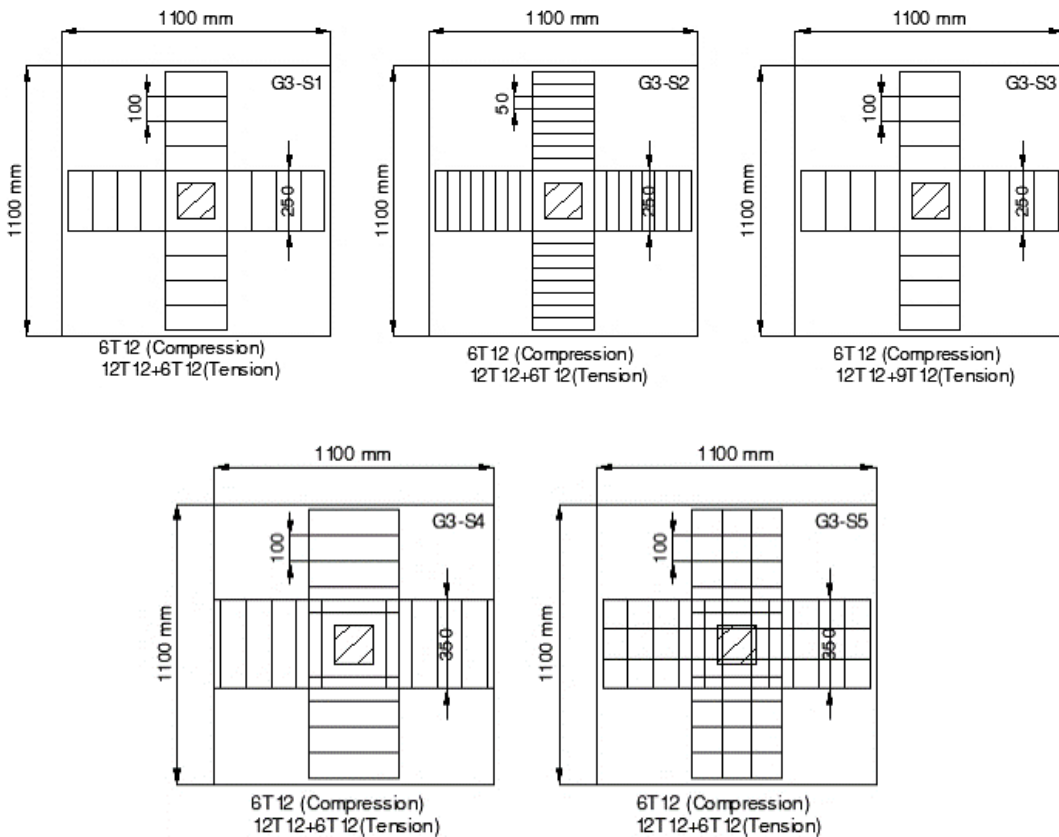


Figure 4. Specimens plans details of group-3 (punching shear reinforcement ratio)

A concrete mix was conducted in order to achieve a concrete cube strength of 35 MPa after twenty-eight days. The concrete mix utilized in design is summarized in Table 2. The average concrete cube results for strength tests are displayed in Table 2. As seen in Figure 5, the specimens are poured in timber square form. A 0.125 m³ mechanically rotating laboratory mixer is employed for mixing. Once the reinforced concrete has been well mixed for approximately four minutes, it is inserted into the form along with ten test cubes and vibrated using an electrical vibrator, as shown in Figure 6.

Table 2. Concrete mix used in design

Mix design used in design	Quantity
Characteristic concrete strength (MPa)	35
Cement (kg/m ³)	375
Fine aggregate (kg/m ³)	650
Coarse aggregate (kg/m ³)	1180
Water (kg/m ³)	200
Water-cement ratio	0.53
Range water reducer BVF (L/m ³)	3.5



Figure 5. Wooden forms used to cast specimens



Figure 6. Specimens casting

2.2. Instruments and Apparatus

Electrical strain gauges were used to measure the strains of the stirrup steel, compression steel, and tension reinforcement. In order to conduct concentric punching shear tests on the slab column connections, the fixed large frame available at the concrete laboratory of Cairo University was used in accordance with the setup shown in Figure 7. The specimens are supported at every one of their four corners by rigid plates. LVDTs were used in this experiment to measure the vertical deflection of the slabs, as shown in Figure 8. Hydraulic jacks capable of supporting 50 tons are used to test the slab specimens under concentric loads. The applied load is progressively increased from zero to the failure load. The load rate is increased incrementally by 0.5 tons until the first initial crack appears; after that, it is increased progressively by 1.0 tons.



Figure 7. Loading setup of the tested specimens



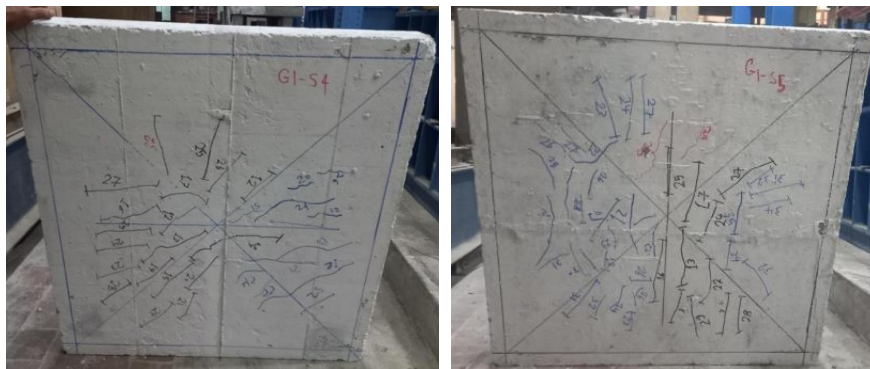
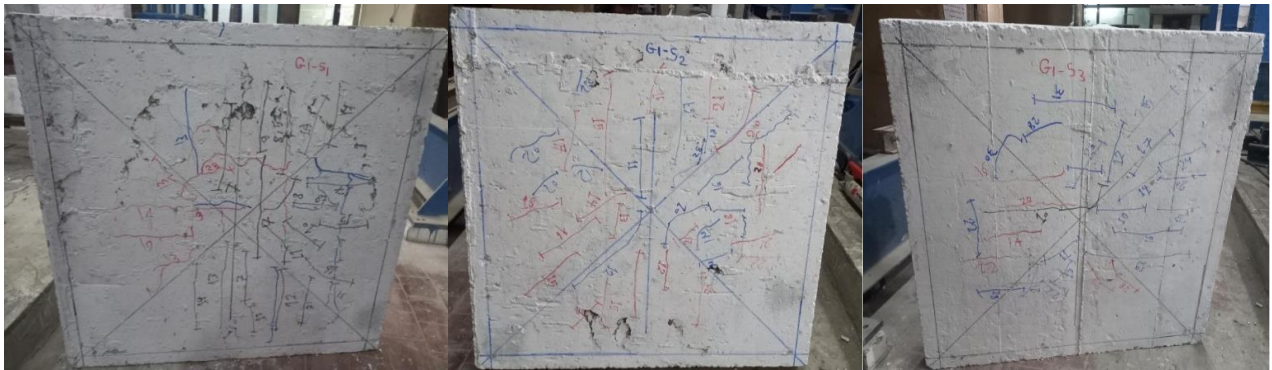
Figure 8. LVDT location

At each loading stage, cracks are inspected and noted if any are found. The experimental configuration is carefully aligned and balanced to allow for any mode of failure. A laptop and a data logger were used to measure and record all of the data concurrently.

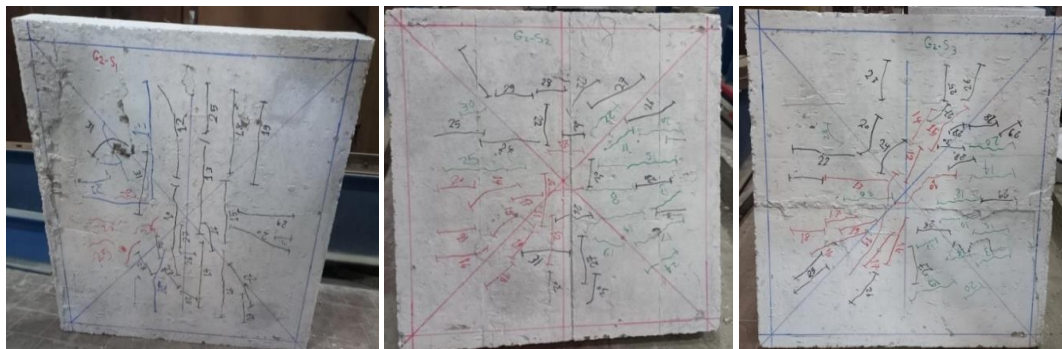
3. Analysis and Discussion of Experimental Results

3.1. Crack Pattern and Mode of Failure

The tested specimens appeared to have typical punching shear-incline cracking in the vicinity of the column. For all tested specimens, the first radial flexural crack is noticed over the column zone area at a cracking load of about 70–125 kN. This behavior is referred to as reaching the concrete tension strength at the tension fiber side of the specimen. Nevertheless, the behavior changes after the appearance of the first flexural crack; as the load increases, the cracks widen and extend towards the slab support, but at different times. In general, the failure occurred at different loads and in different shapes, but the loud sound of the failure is common in all groups of specimens. Figures 9-a, 9-b, and 9-c show the crack patterns for tested specimens. The mechanism of failure of all tested specimens is regarded as brittle failure, as shown in Figure 10.



(a)



(b)

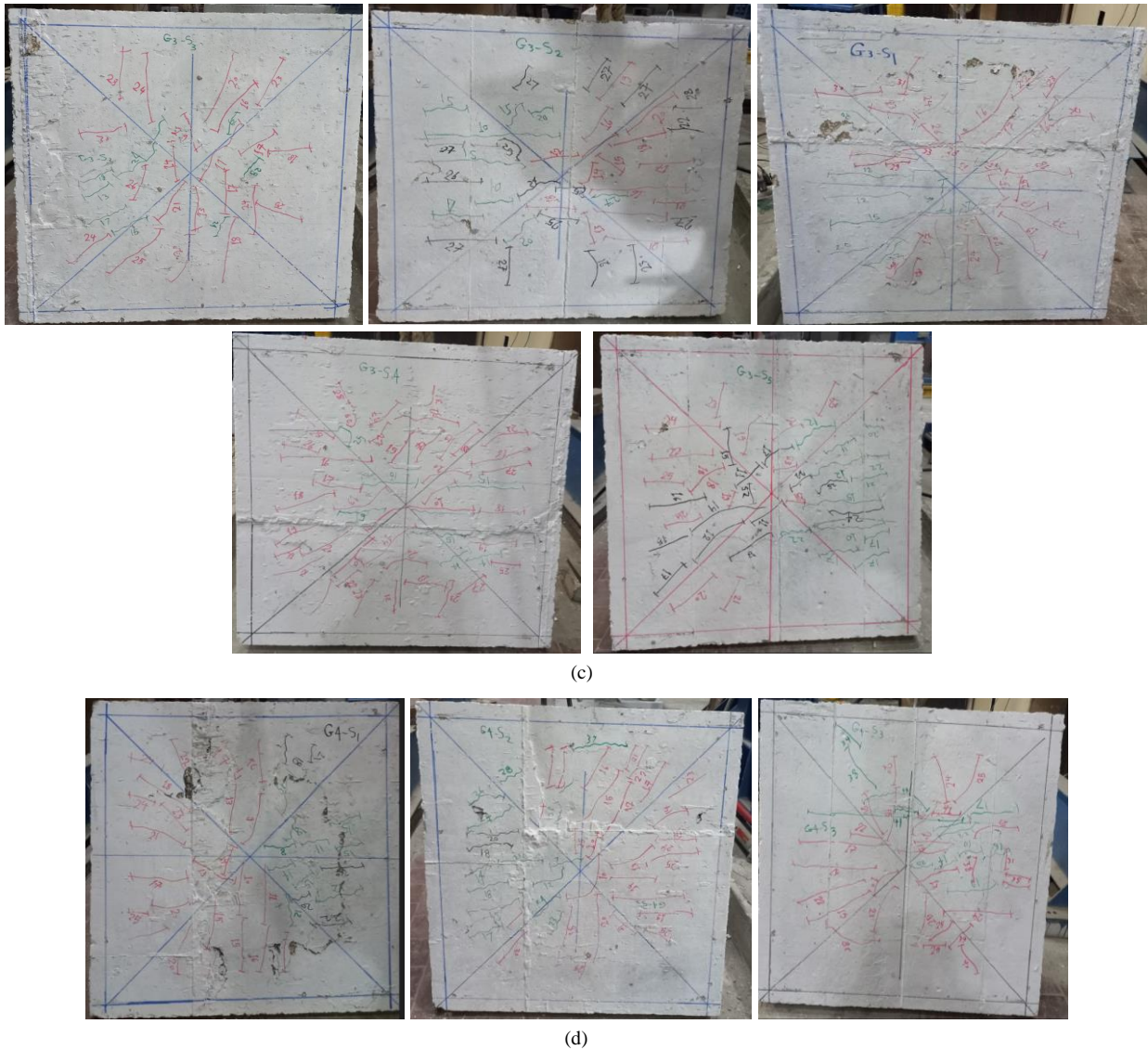


Figure 9. (a) Crack pattern and mode of failure for group – 1, (b) Crack pattern and mode of failure for group - 2, (c) Crack pattern and mode of failure for group - 3, (d) Crack pattern and mode of failure for concrete compressive strength group

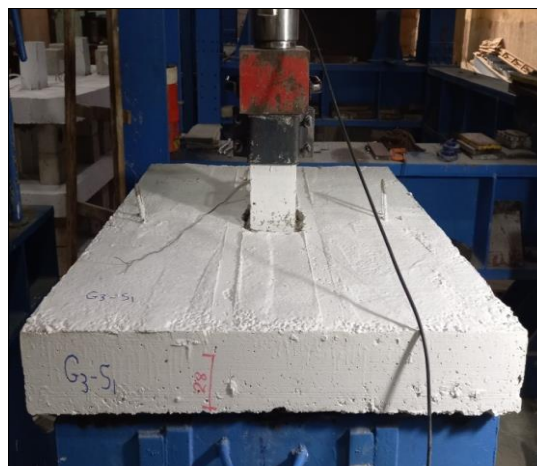


Figure 10. Typical mode of failure of specimens

For more accurate results, three specimens were added with variable concrete cube compressive strength as shown in Figure 10. The specimen (G4-S1) with cube compressive strength equal to 35 MPa, the specimen (G4-S2) with 40 MPa, and the specimen (G4-S3) with a strength 45 MPa. The failure shapes as shown in Figure 9-d, the failure load was 321 kN for (G4-S1), the failure load was 397 kN for (G4-S2), and the failure load was 421 kN for (G4-S3). The punching shear strength increased by about 31% due to increasing the compressive strength.

In the case of specimen G3-S3, radial cracking propagated normally from the column toward the supports, as shown in Figure 11. However, premature failure occurred at the support. This kind of failure may be attributed to the high punching capacity of this specimen, which caused an unexpected failure at the slab corners. Specimens G3-S3 had the largest tension reinforcement, with stirrups compared to other specimens at punching shear reinforcement ratio group.



Figure 11. mode of failure of specimen G3-S3

3.2. Load-Deflection Response of Group 1

The relation between load and deflection, as shown in Figure 12, is compared for the five tested slabs. Table 3 illustrates the initial crack load, and the maximum deflection at the ultimate load, as well as the failure load on each slab.

Table 3. Summary of load-deflection for tested specimens (Group 1)

Specimen	Crack load (kN)	Deflection (mm)	Ultimate load (kN)
G1-S1	70	8.83	280
G1-S2	80	9.97	300
G1-S3	90	7.69	307.3
G1-S4	100	7.88	320
G1-S5	120	8.52	357

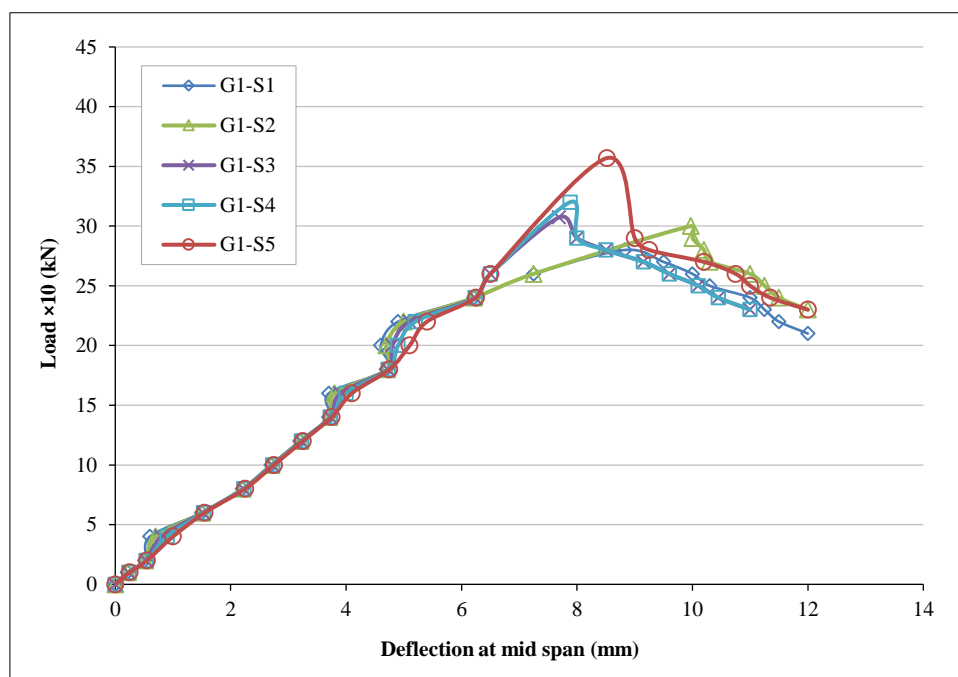


Figure 12. Load-deflection curve of Group-1

The tested specimen G1-S5 is higher than other specimens regarding the ultimate load. The maximum load increased by 7%, 9.7%, 14%, and 27.5% for specimens G1-S2, G1-S3, G1-S4, and G1-S5, respectively, compared to control slab G1-S1.

The curve generally showed a linear behavior from the beginning of the loading till the appearance of the initial crack load (P_{cr}), and after that the curve showed a non-linear behavior till the maximum load value. The ultimate load and corresponding deflection values increased due to the increasing flexural reinforcement ratio, as shown in Figure 12. The load-increasing value was between 280 and 357 kN.

3.3. Load-Deflection Response of Group 2

The relation between deflection and load, as shown in Figure 13, is compared for the five tested slabs. Table 4 illustrates the initial crack load, the maximum deflection, and the failure load for every specimen.

Table 4. Summary of load-deflection for tested specimens (Group 2)

Specimen	Crack load (kN)	Deflection (mm)	Ultimate load (kN)
G2-S1	75	8.21	316.8
G2-S2	85	6.21	328.1
G2-S3	110	9.22	331.6
G2-S4	120	10.68	338
G2-S5	115	10.00	335

The tested specimen G2-S5 is higher than other specimens regarding the ultimate load. The maximum load increased by 3.5%, 4.6%, 5.7%, and 6.69% for specimens G2-S2, G2-S3, G2-S4, and G2-S5, respectively, compared to control slab G2-S1.

The curve generally showed a linear behavior from the beginning of the loading till the appearance of the initial crack load (P_{cr}), and after that the curve showed a non-linear behavior till the maximum load value. The ultimate load and associated deflection measurements increased due to the compression reinforcement, as seen in Figure 13. The load rising was between 316.80 and 338 kN in value.

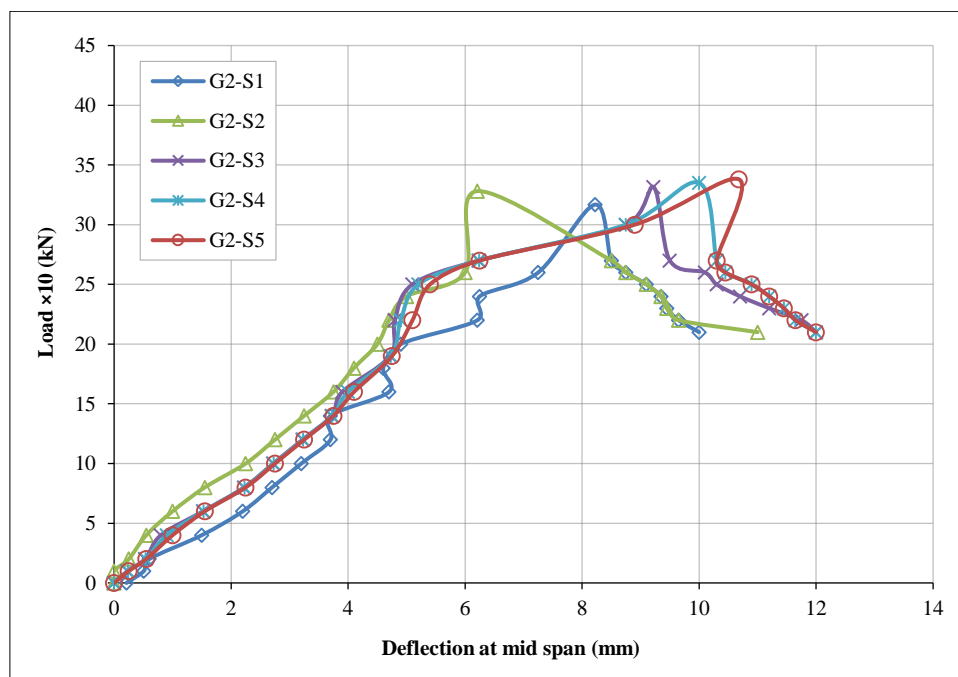


Figure 13. Load - deflection curve of Group-2

3.4. Load-Deflection Response of Group 3

The relationship between the deflection and the load, as shown in Figure 14, is compared for the five tested specimens. Table 5 illustrates the initial crack load, the maximum deflection, and the failure load for every slab.

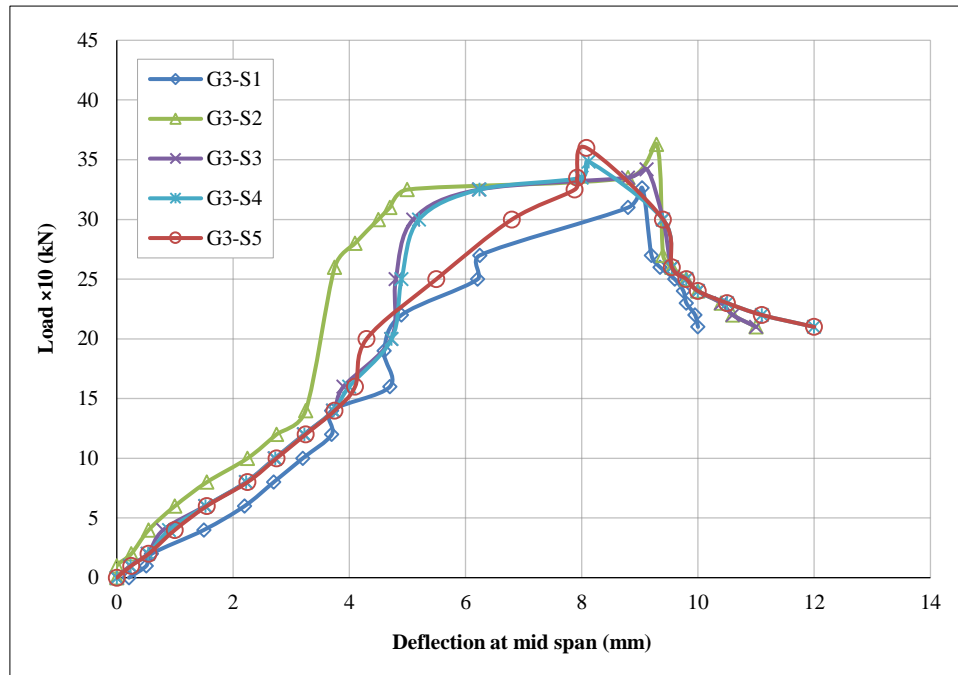


Figure 14. Load-deflection curve of Group-3

Table 5. Summary of load-deflection for tested specimens (Group 3)

Specimen	Crack load (kN)	Deflection (mm)	Ultimate load (kN)
G3-S1	85	9.04	326.4
G3-S2	100	9.29	362.9
G3-S3	115	9.12	342.1
G3-S4	120	8.4	345.8
G3-S5	125	8.08	360

The tested specimen G3-S5 is higher than other specimens regarding the ultimate load. The maximum load increased by 11%, 4.8%, 5.9%, and 10% for specimens G3-S2, G3-S3, G3-S4, and G3-S5, respectively, compared to control slab G2-S1.

The curve generally showed a linear behavior from the beginning of the loading till the appearance of the initial crack load (P_{cr}), and after that the curve showed a non-linear behavior till the maximum load value.

The cracking and ultimate punching capacities of all the tested specimens are presented in Figures 15 to 17. It can be seen from the figure that the largest cracking load was recorded in specimens G1-S5, G2-S4, and G3-S2. Specimen G1-S5 is the specimen with the highest flexural reinforcement ratio. Slab G2-S4 has the highest compression reinforcement ratio. Slab G3-S2 is the specimen with the highest amount of stirrups, with a width of 250 mm and a distance between stirrups of 50 mm.

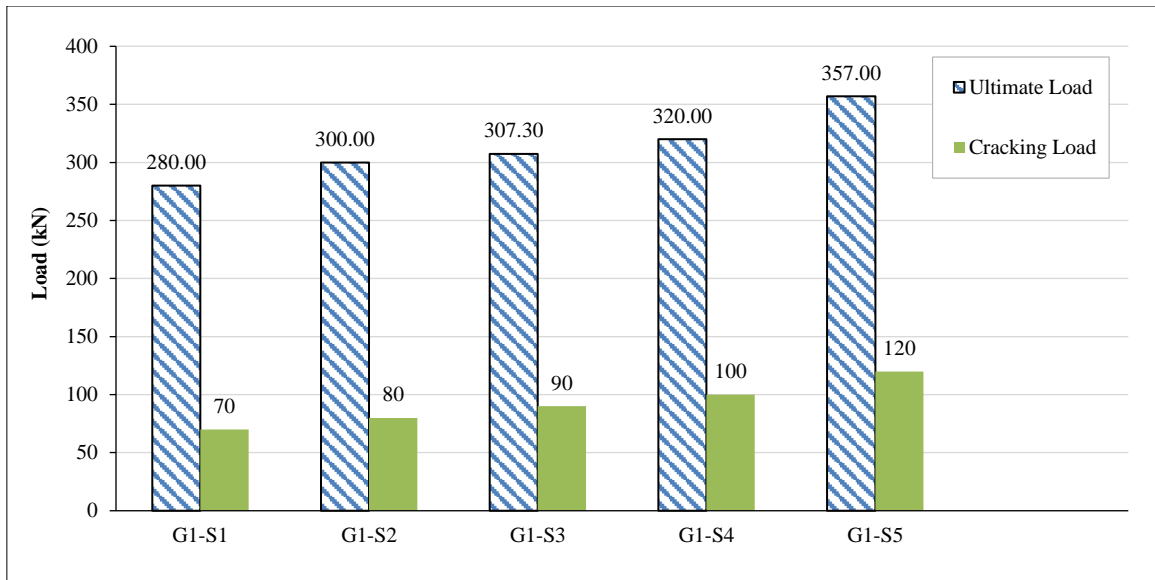


Figure 15. Cracking load and ultimate punching capacity of the tested slabs – Flexural reinforcement ratio

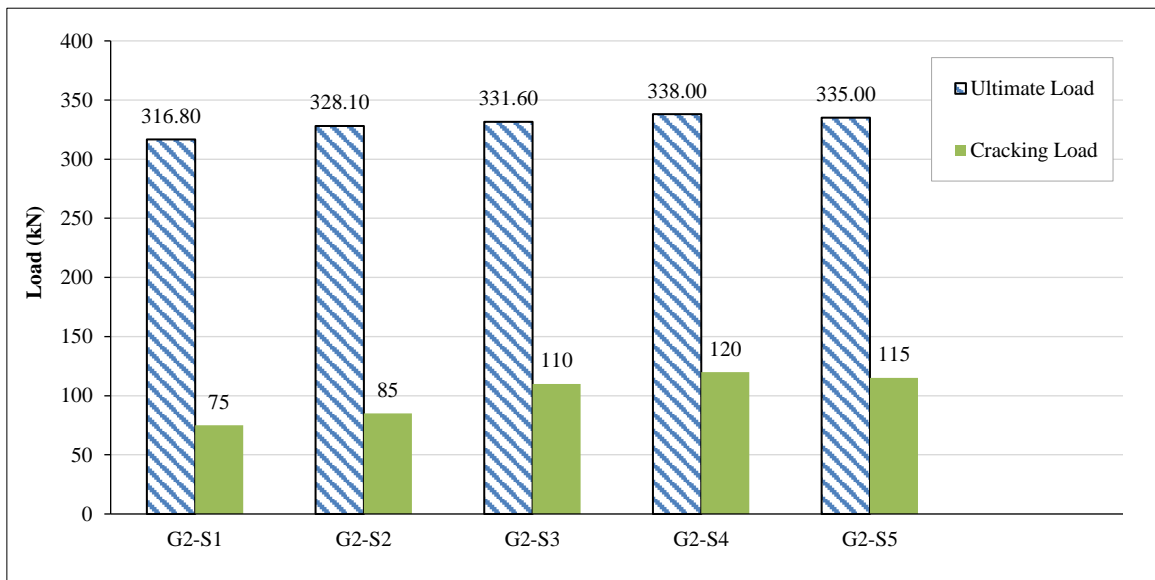


Figure 16. Cracking load and ultimate punching capacity of the tested slabs – Compression reinforcement ratio

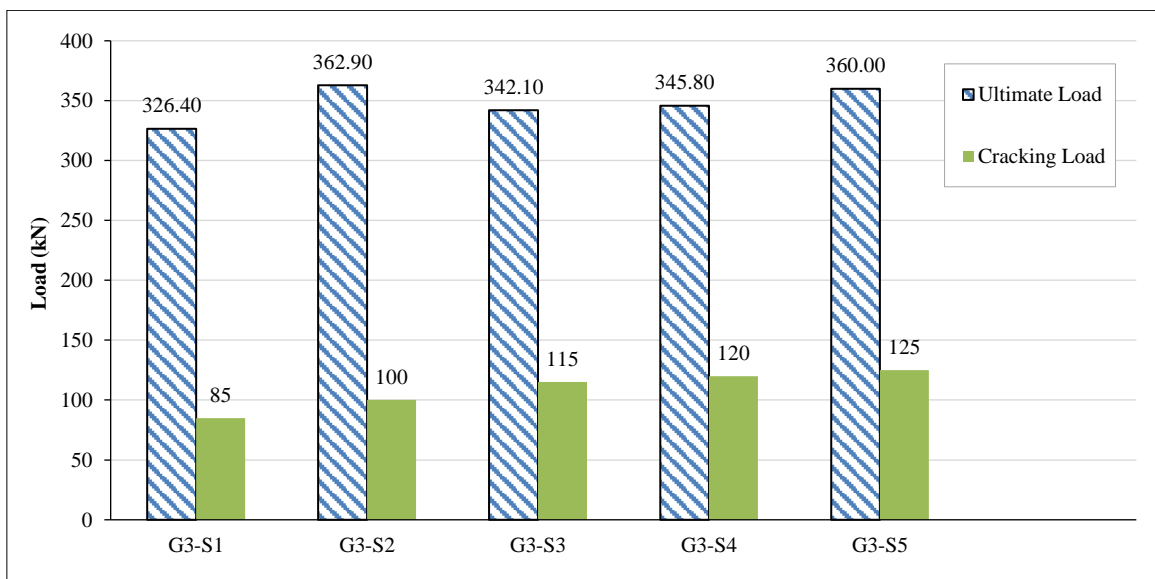


Figure 17. Cracking load and ultimate punching capacity of the tested slabs – Stirrups reinforcement ratio

3.5. Steel Strain

Figure 18 shows the load-strain relationship for slabs G1-S1, G1-S4, and G1-S5, where strain was measured in the flexural reinforcement. The steel of specimen G1-S1 reached the yield stress at an applied load of 230 kN, while the flexural reinforcement in specimens G1-S4 and G1-S5 with higher reinforcement ratios did not reach the yield strain.

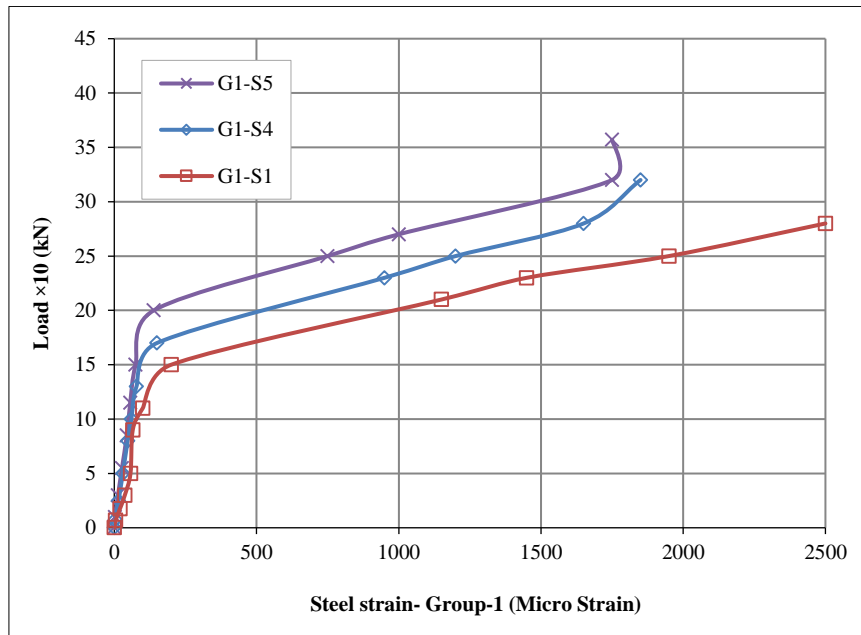


Figure 18. Load-strain curve for Specimens-Flexural reinforcement ratio

Figure 19 shows the load-strain relationship for slabs G2-S1, G2-S3, and G2-S4, where strain was measured in the compression reinforcement. The steel of specimen G2-S1 reached the yield stress at an applied load of 280 kN, while the compression reinforcement in specimens G2-S3 and G2-S4 with higher compression reinforcement ratios did not reach the yield strain.

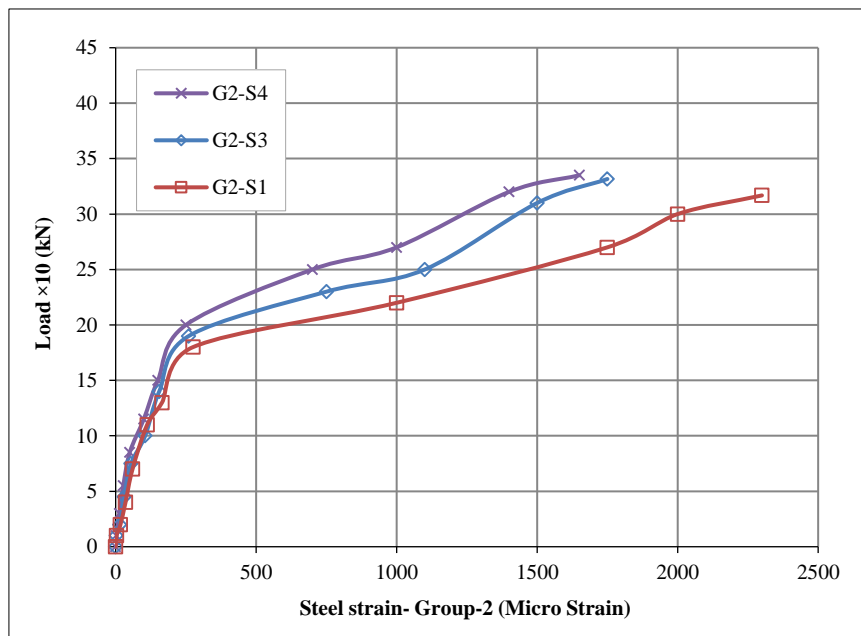


Figure 19. Load-strain curve for specimens-Compression reinforcement ratio

Figure 20 shows the load-strain relationship for the vertical stirrups in specimens G3-S1 and G3-S2. Both of these specimens had stirrups with spacings of 100 mm and 50 mm, respectively. The strain was measured at one branch of the stirrup located at $d/2$ from the face of the column, where d is the effective depth of the slab. It can be seen that the strain and consequently the stress are higher in slab G1-S1 with stirrup spacing of 100 mm.

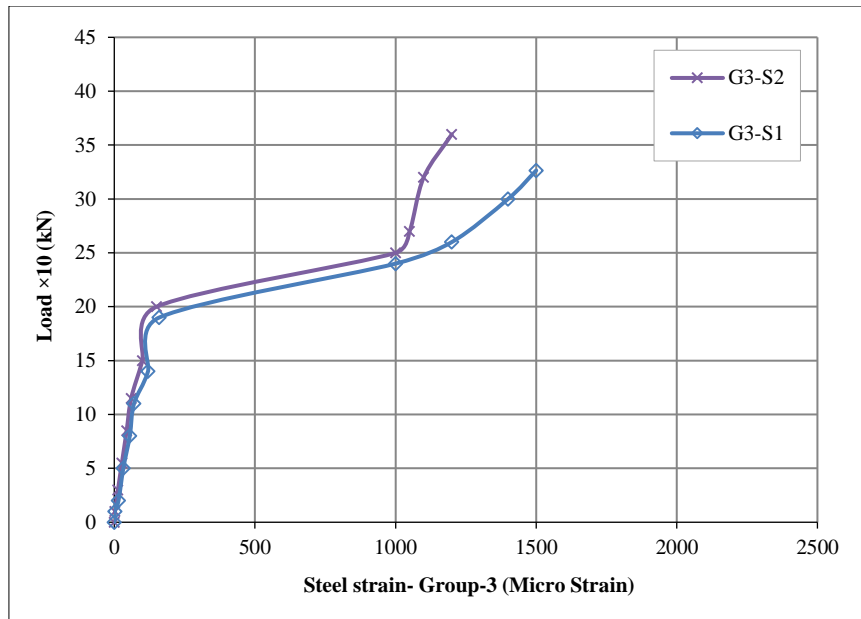


Figure 20. Load-strain curve for specimens-Stirrups reinforcement ratio

4. Design of Punching with Different Standard Codes

This section will cover the design techniques for punching according to standard codes of design; Egyptian ECP 203 edition 2020 [1], ACI 318 edition 2019 [2], and Euro code 2 edition 2004 [3].

4.1. Egyptian Standard Concrete Code (ECP NO-203 Edition 2020)

Maximum punching stress (q_{up}) without providing punching reinforcement shall be calculated by:

$$q_{up} \leq q_{cup} \tag{1}$$

$$q_{up} = \frac{Q_{up}}{b_0 d} \tag{2}$$

$$q_{cup} = 0.316 \sqrt{\frac{f_{cu}}{\gamma_c}} \leq 1.7 \text{ MPa} \tag{3}$$

where: Q_{up} is the ultimate shear force, q_{cup} is concrete punching strength, f_{cu} concrete cube compressive strength, γ_c is the concrete reduction factor equal 1.5, and b_0 is the punching perimeter at distance equal half of the effective slab depth from the face of the concrete column.

The ultimate capacity punching stress (q_{up}) with punching reinforcement would be determined by:

$$q_{up} = 0.12 \sqrt{\frac{f_{cu}}{\gamma_c}} + \frac{A_{st} f_y}{s b_0 \gamma_s} \leq 0.45 \sqrt{\frac{f_{cu}}{\gamma_c}} \tag{4}$$

where f_y is the punching reinforcement yield strength, s is the radial spacing between stirrups, A_{st} is the total section area of punching reinforcement on a single peripheral line, and γ_s is the reduction factor for reinforcing steel equal to 1.15.

4.2. The Standard American Code ID (ACI 318 Edition 2019)

Nominal shear strength without punching reinforcement will be determined by:

$$v_u \leq \phi v_n \tag{5}$$

$$v_c = 0.33 \sqrt{f_c'} \tag{6}$$

where f_c' is the cylindrical concrete strength at compression (MPa), v_u is the maximum shear stress, v_n is the nominal shear stress, and v_c is the nominal shear stress provided by concrete.

Nominal punching strength with vertical reinforcement to be determined by:

$$v_n = 0.17 \sqrt{f_c'} + \frac{A_v f_y t}{b_o s} \leq 0.5 \phi \sqrt{f_c'} \tag{7}$$

The following is a clear statement of the essential requirements for punching strength design:

Design strength, $\emptyset v_n \geq$ required strength, vu ; where \emptyset is the reduction factor for punching equal to 0.75. For flat slabs, punching force v_u is computed using the following Equation:

$$v_u = v_n b_0 d \quad (8)$$

4.3. Euro Code 2: British Standard BS Edition 1992

The design punching shear strength [MPa] for slabs without punching reinforcement may be calculated as follows:

$$v_{Rd,c} = c_{Rd,c} k (100 \rho_1 f_{ck})^{\frac{1}{3}} \geq V_{min} = 0.035 k^{3/2} f_{ck}^{1/2} \quad (9)$$

where:

$$c_{Rd,c} = \frac{0.18}{\gamma_c} \quad (10)$$

γ_c is the reduction factor equal 1.50; k is a dimensionless factor that considers the size effect and is defined by the following Equation:

$$k = 1 + \sqrt{\frac{200}{d}} \leq 2 \quad (11)$$

$$\rho_1 = \sqrt{\rho_1 y \rho_1 z} \leq 0.02 \quad (12)$$

where γ_c is the reduction factor where equal to 1.5, and $v_{Rd,c}$ is the design shear strength of the member without punching reinforcement, ρ_1 is the reinforcement ratio for longitudinal reinforcement, $\rho_1 y$ and $\rho_1 z$ are the proportion of the flexural reinforcement in both directions, and f_{ck} is the cylindrical concrete compressive strength (MPa).

The strength of punching of slabs provided by shear reinforcement will be calculated by using the following Equation:

$$v_{Rd,cs} = 0.75 V c_{Rd,c} + 1.5 \left(\frac{d}{s_r} \right) A_{sw} f_{ywd,ef} \left(\frac{1}{u_1 d} \right) \sin \alpha \quad (13)$$

where: $v_{Rd,cs}$ is the design shear strength of the member with punching reinforcement, A_{sw} is the shear steel area on one edge of the concrete column (mm^2), s_r is the radial distance between the shear reinforcement perimeter (mm), $f_{ywd,ef}$ is the effective design strength of punching reinforcement in MPa, according to:

$$f_{ywd,ef} = 250 + 0.25d \leq f_{ywd}, \quad (14)$$

f_{ywd} is the design yield strength for punching shear reinforcement, u_1 is the length of the main control perimeter, and α is the angle between the shear reinforcement and the plane of the slab.

At the column perimeter, or the perimeter of the loaded area, the maximum punching shear stress should not be exceeded:

$$v_{Ed} < VRd, max = 0.5 \times 0.6 \left(1 - \frac{f_{ck}}{250} \right) \times f_{cd} / 250 \quad (15)$$

where: VRd, max is is the design value of the maximum shear force which can be sustained by the member, limited by crushing of the compression struts, f_{ck} is the cylinder compressive strength of concrete at 28 days, and f_{cd} is the compressive strength of concrete design value.

The applied shear force design value adjacent to column V_{Ed} is to be determined as follows:

$$V_{Ed} = v_{Ed} \cdot u_o \cdot \frac{d}{\beta} \quad (16)$$

where: u_o for an interior column, u_o is the column length perimeter (mm), and β is the factor for position of column, for internal column equal to 1.15.

5. Comparison of the Experimental Results with the Design Codes

The aim of comparison between the punching shear strength recorded from the tested specimens and the strength calculated from standard codes in order to determine how these codes are close to the experimental results. Some similarities can be noted by comparing the codes equations. All previous codes reduce the punching strength of concrete slabs. Thus this value is reduced for 52% in ECP 203-2020, 57% in ACI 318-19, and 33% in Euro code 2.

Figures 15 also shows that the largest punching capacity was obtained in slab G1-S5, which is again the slab with the highest flexural reinforcement ratio. Figures 16 also shows that the largest punching capacity was obtained in slab G2-S4, which is again the slab with the highest compression reinforcement. Figures 16 also shows that the largest punching capacity was obtained in slab G3-S2, which is again the slab with the highest vertical stirrup reinforcement with a distance 50 mm.

The comparison in Table 6 showed that the values estimated according to codes are generally conservative. It can be seen that the conservative level increased by increasing the percentage of the flexural reinforcement ratio. This ratio reaches a value above 2 in the case of specimen G1-S5, which has the highest reinforcement ratio when compared to values estimated by ECP (203–2020) and ACI (318–19).

Table 6. Comparison of experimental results with values calculated of design codes

Specimen	Pu (kN) Experimental	Pu(kN) ECP	Pu(kN) ACI	Pu(kN) Euro: BS	Pu-Exp./Pu-code		
					ECP	ACI	BS
G1-S1	280	153	131	177	1.83	2.14	1.58
G1-S2	300	153	131	191	1.96	2.29	1.57
G1-S3	307.3	153	131	202	2.01	2.35	1.52
G1-S4	320	153	131	202	2.09	2.44	1.58
G1-S5	357	153	131	202	2.33	2.73	1.77
G2-S1	316.8	153	131	202	2.07	2.42	1.57
G2-S2	328.1	153	131	202	2.14	2.50	1.62
G2-S3	331.6	153	131	202	2.17	2.53	1.64
G2-S4	338	153	131	202	2.21	2.58	1.91
G2-S5	335	153	131	177	2.19	2.56	1.66
G3-S1	326.4	142	140	254	2.30	2.33	1.29
G3-S2	362.9	226	212	356	1.61	1.71	1.02
G3-S3	342.1	142	140	254	2.41	2.44	1.35
G3-S4	345.8	142	140	254	2.44	2.47	1.36
G3-S5	360	226	212	356	1.59	1.70	1.01
Average value					2.09	2.35	1.50

As for ECP (203–2020) and ACI (318–19), the ultimate capacity for concrete was the governing value in the tested slabs without punching shear reinforcement. It can also be seen that the ECP code and ACI code gave values that underestimated the punching capacity of the slabs but were still more conservative than those in the Euro code. This is due to the fact that the Euro code takes the effect of flexural reinforcement into account when punching, while the ECP code and ACI code neglect the contribution of flexural reinforcement.

6. Proposed Equation Guided to ACI 318 Edition 2019 Code

The US code ACI318-19 [2] ignores the contribution of slabs flexural reinforcement on punching shear strength. As a result, the punching strength is conservative in the ACI code. From this standpoint, guided by the outcomes of the experimental program and an Excel spread sheets, a new equation derived from the American code was proposed after adding the effect of flexural reinforcement to be less conservative and closer to the experimental program. Equation 17 is related to ultimate punching shear without punching shear force, and the Equation 18 is related to ultimate punching shear force with punching reinforcement.

$$V_c = 0.46(\rho_t f_{yt} \sqrt{f_c'})^{0.5} \times bo \times d \quad (17)$$

$$V_n = 0.23(\rho_t f_{yt} \sqrt{f_c'})^{0.5} + \left(\frac{A_v f_{yt}}{bo s}\right) \times (bo \times d) \quad (18)$$

where: (ρ_t) is the longitudinal reinforcement ratio at tension side, (bo) is the punching perimeter, and (d) is the effective depth of slab.

7. Conclusions

Considering the experimental results, the following conclusions can be summarized:

- The failure of all the tested specimens was a brittle punching shear failure.
- Adding vertical shear reinforcement in the form of stirrups improved the punching capacity of the slabs by 7% in the case of spacing 100 mm and 18% in the case of spacing 50 mm. Providing stirrups in the two directions of the slab with a stirrup width equal to the column width plus slab thickness was effective in enhancing the punching behavior of the slabs.
- Increasing the width of stirrups to be equal to column width plus twice the thickness instead of column width plus the thickness caused a slight increase in the punching strength.
- The flexural reinforcement in a flat slab contributes to the punching capacity of the slab. As the flexural reinforcement ratio was increased by 25%, the punching capacity increased by 7%; when the reinforcement ratio was increased by 50% compared to the control specimen (G1-S1), the increase in the punching capacity was 10%; when the reinforcement ratio was increased by 75% compared to the control specimen (G1-S1), the increase in the punching capacity was 15%; and when the reinforcement ratio was increased by 100% compared to the control specimen (G1-S1), the increase in the punching capacity was 28%.
- The compression reinforcement in a flat slab contributes to the punching capacity of the slab. As the compression reinforcement ratio was 33% from the flexural reinforcement, the punching capacity increased by 3%, and when the reinforcement ratio was increased 50% from the flexural reinforcement, the increase in the punching capacity was 7%, and when the reinforcement ratio was increased 67% from the flexural reinforcement, the increase in the punching capacity was 8%, and when the reinforcement ratio was increased 83% compared to the control specimen (G1-S3), the increase in the punching capacity was about 10%.
- Increasing the concrete compressive strength for tested specimens improved the punching behavior and increased the punching strength by about 30%.
- The punching capacities estimated according to the E.C.P. (203–2020) and the ACI 318–19 are generally less than those that resulted from tests and experiments. The ACI code is more conservative than the Egyptian code in estimating the punching shear capacity.
- The punching capacities estimated according to the Euro code -2 are less conservative than the Egyptian code, and the ACI code, due to the Euro code -2, takes the flexural reinforcement ratio into consideration, while both other codes neglect the contribution of tension reinforcement.
- The comparison of experimental results with the design standard codes ECP 203-2020 and ACI 318-19 reveals that both design codes overstate the reduction of the shear strength of slabs, with an average increase of 109% for code ECP 203 and 135% for code ACI 318, while Euro code 2 has an average increase of 50%.
- The ACI 318 standard equations for the punching shear strength of interior slab-column connections should be modified to take the ratio of flexural reinforcement on the punching shear strength of flat slabs.

8. Declarations

8.1. Author Contributions

Conceptualization, A.A. and M.R.; analytical and analysis, A.A. and M.R.; analysis and interpretation of the results, A.A.; writing—original draft preparation, A.A. and M.R.; writing—review and editing, A.A. and M.R. All authors have read and agreed to the published version of the manuscript.

8.2. Data Availability Statement

The data presented in this study are available on request from the corresponding author.

8.3. Funding

The authors received no financial support for the research, authorship, and/or publication of this article.

8.4. Conflicts of Interest

The authors declare no conflict of interest.

9. References

- [1] E.C.P.-203 (2007) Egyptian Code for Design and Construction of Reinforced Concrete Structures. National Housing and Building Research Center, Giza, Egypt.
- [2] ACI 318-19. (2019). Building Code Requirements for Structural Concrete (ACI 318-19) and Commentary (318R-19), American Concrete Institute (ACI), Michigan, United States. doi:10.14359/51716937.
- [3] EN 1992-1-1. (2004). Design of Concrete Structures, Part 1–1: General Rules and Rules for Buildings. European Committee for Standardization, Brussels, Belgium, 2004.
- [4] Kinnunen, S., & Nylander, H. S. E. (1960). Punching of concrete slabs without shear reinforcement. Transactions, No. 158, Royal Institute of Technology, Stockholm, Sweden.
- [5] Meisami, M. H., Mostofinejad, D., & Nakamura, H. (2014). Strengthening of flat slabs with FRP fan for punching shear. Composite Structures, 119, 305–314. doi:10.1016/j.compstruct.2014.08.041.
- [6] Ebead, U. A. A. (2002). Strengthening of reinforced concrete two-way slabs. Ph.D. Thesis, Memorial University of Newfoundland, St. John's, Canada.
- [7] Megally, S. H. (1998). Punching shear resistance of concrete slabs to gravity and earthquake forces. Ph.D. Thesis, University of Calgary, Calgary, Canada.
- [8] Brooms, C. E. (1990). Shear reinforcement for deflection ductility of flat plates. ACI Structural Journal, 87(6), 696–705. doi:10.14359/2988.
- [9] Mabrouk, R. T. S., Bakr, A., & Abdalla, H. (2017). Effect of flexural and shear reinforcement on the punching behavior of reinforced concrete flat slabs. Alexandria Engineering Journal, 56(4), 591–599. doi:10.1016/j.aej.2017.05.019.
- [10] Raafat, A., Fawzi, A., Metawei, H., & Abdalla, H. (2021). Assessment of stirrups in resisting punching shear in reinforced concrete flat slab. HBRC Journal, 17(1), 61–76. doi:10.1080/16874048.2021.1881422.
- [11] Abdel-Rahman, A. M., Hassan, N. Z., & Soliman, A. M. (2018). Punching shear behavior of reinforced concrete slabs using steel fibers in the mix. HBRC Journal, 14(3), 272–281. doi:10.1016/j.hbrj.2016.11.001.
- [12] Afifi, A., Ramadan, M., Farghal Maree, A. M., Ebid, A. M., Zaher, A. H., & Ors, D. M. (2023). Punching Capacity of UHPC Post Tensioned Flat Slabs with and Without Shear Reinforcement: An Experimental Study. Civil Engineering Journal (Iran), 9(3), 567–582. doi:10.28991/CEJ-2023-09-03-06.
- [13] Ramadan, M., Ors, D. M., Farghal, A. M., Afifi, A., Zaher, A. H., & Ebid, A. M. (2023). Punching shear behavior of HSC & UHPC post tensioned flat slabs – An experimental study. Results in Engineering, 17, 100882. doi:10.1016/j.rineng.2023.100882.
- [14] Nguyen, K. Le, Trinh, H. T., & Pham, T. M. (2024). Prediction of punching shear strength in flat slabs: ensemble learning models and practical implementation. Neural Computing and Applications, 36(8), 4207–4228. doi:10.1007/s00521-023-09296-0.
- [15] Khaloo, A., Borhani, M. H., Habibi, O., Tabatabaeian, M., & Askari, S. M. (2024). Experimental and numerical investigation on the performance of GFRP-confined expansive concrete-filled unplasticized polyvinyl chloride tubes. Journal of Thermoplastic Composite Materials, 37(3), 983–1011. doi:10.1177/08927057231190558.
- [16] Habibi, O., Youssef, T., Naseri, H., & Ibrahim, K. (2024). Ensemble Learning Models for Prediction of Punching Shear Strength in RC Slab-Column Connections. Civil Engineering Journal, 10, 1–20. doi:10.28991/cej-sp2024-010-01.